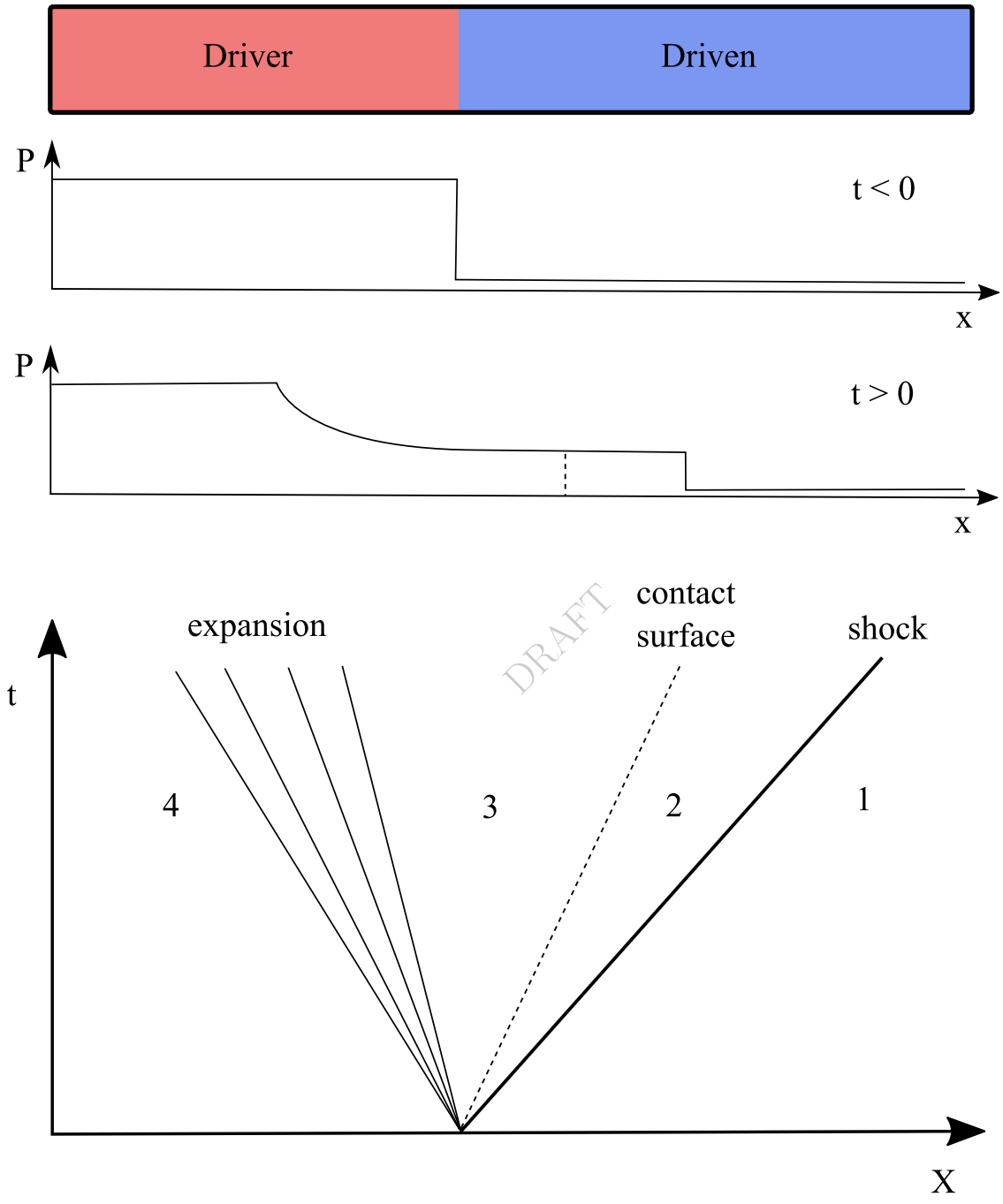

Figure 7.17: Conventional shock tube and initial wave system generated by diaphragm rupture.

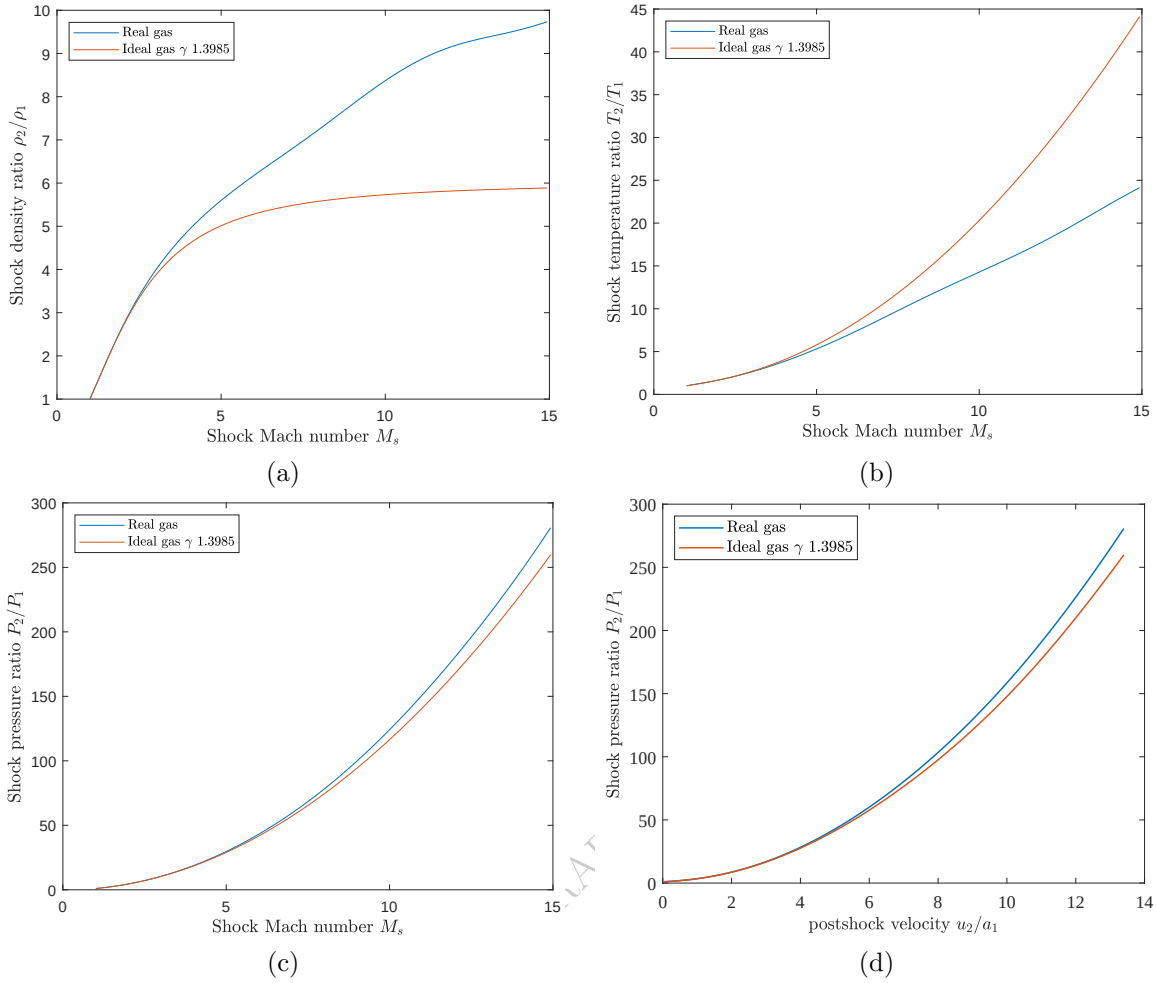

Figure 7.18: Equilibrium postshock properties: (a) density, (b) temperature, (c) pressure as a function of shock Mach number and (d) Pressure-velocity relationship. Air at an initial state of 1 bar and 298.15 K.

The solution for states 2 and 3 for given values of states 1 and 4 is found by requiring that pressure and velocity are continuous at the contact surface between these states

$$u_2 = u_3 \ , \tag{7.146}$$

$$P_2 = P_3 \ . \tag{7.147}$$

The solution proceeds by tabulation of $P(u)$ for states 2 and 3 followed by interpolation and a simple root-finding routine. This can be graphically visualized as finding the intersection of the shock and expansion wave curves in the P-u plane. The ideal gas solutions of Appendix A.11 are a useful first approximation, particularly for expansion waves in the driver but for strong shock waves with rapid equilibration behind the front, the shock and detonation toolbox equilibrium postshock routines give more realistic answers. At shock Mach numbers greater than about 3 in air initially at 1 bar pressure, dissociation results in significant changes in composition and departures of the gas density and temperature from ideal gas values, less significant are the departures of the $P(u)$ relationship from ideal.

Examples of wave curves and solutions for states 2 and 3 are shown in Fig. 7.19 for four types of drivers. The driven gas is air with a composition O_2:0.2095 N_2:0.7808 Ar:0.0093 CO_2:0.0004 and initial state of 100 kPa and 298.15 K. The driver in case (a) is high presure (3.3 MPa) helium. The driver gas used in cases (b), (c), and (d) is a rich propane-oxygen (C_3H_8:2.0 O_2:5.0) mixture with an initial state of 1 bar and 298.15

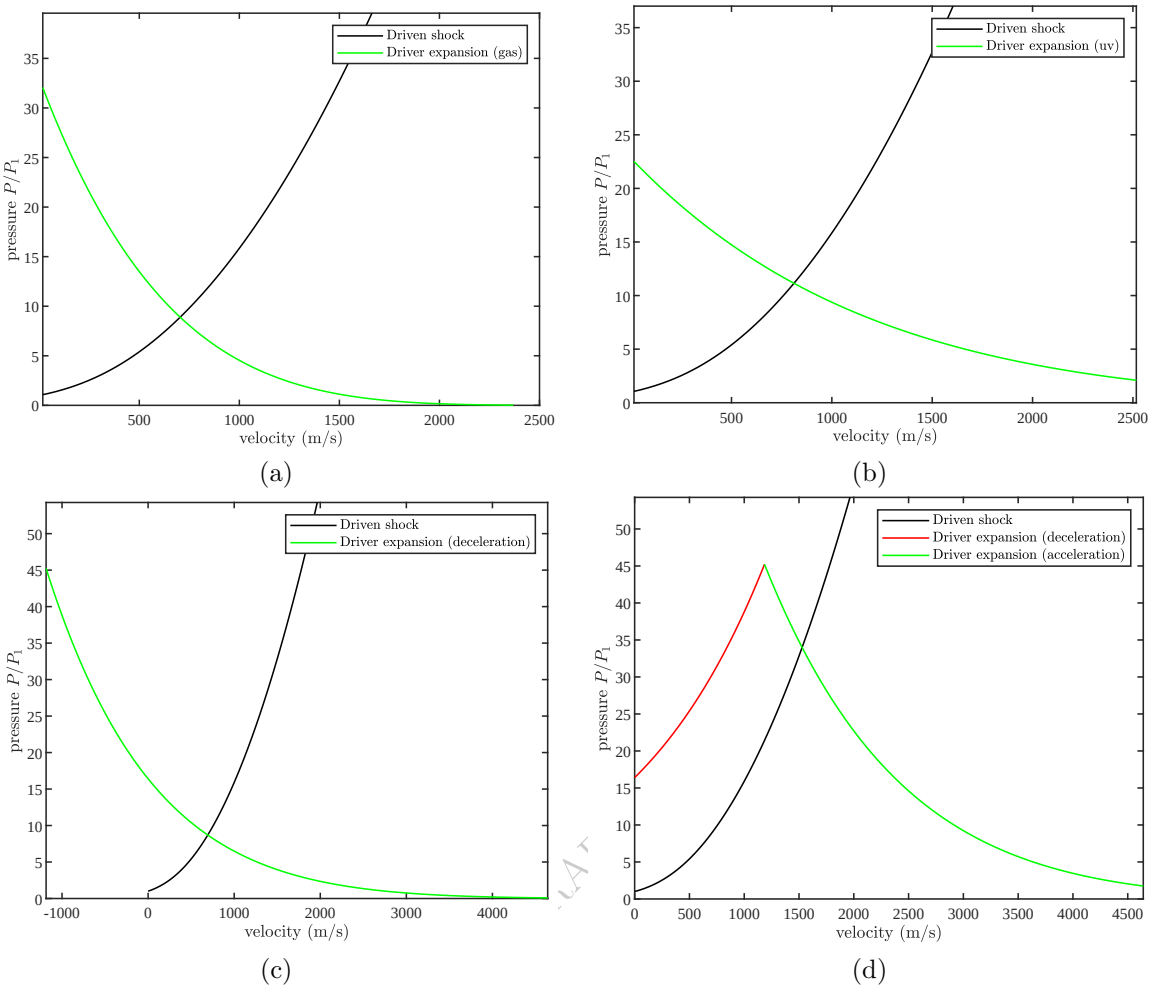

Figure 7.19: Wave curves and solutions for four types of drivers: (a) He ; (b) constant volume explosion of propane-oxygen; (c) reverse (propagation away from diaphragm) detonation of mixture used in case (b); (d) forward (propagation toward diaphragm) detonation of mixture used in case (b).

K. In case b, the driven state is uniform and at the condition of an adiabatic, constant-volume explosions ($P = 2.28$ MPa, $T = 3299$ K). For cases (c) and (d), the conditions are for a detonation wave ($P_{CJ} = 4.52$ MPa, $T_{CJ} = 3540$ K) in the mixture used in case (b). For case (c), the plateau state ($P = 1.64$ MPa, $T = 3103$ K) at the end of the Taylor-Zeldovich wave is most relevant for estimating the driver initial state. The solutions for case (d) only apply immediately after the interaction of the detonation wave with the driver gas as there are significant nonsteady processes associated with the Taylor-Zeldovich expansion flow behind the wave. In cases (a), (b) and (c), the solutions for pressure and velocity at the 2-3 interface are only valid until the reflected expansion wave from the driver end reaches the interface.

There is another case, Fig. 7.20, that occurs when the CJ state lies under the shock wave curve; a reflected shock wave occurs in the driver gas. The interaction of a detonation wave with a contact surface within and at the exit of a detonation tube was investigated numerically and experimentally Wintenberger et al. (2003), Wintenberger (2004) and used in the development of models for pulse detonation propulsion systems. The performance of combustion and detonation-driven shock tubes has been investigated for use in hypervelocity flow facilities (shock tunnels and expansion tubes) Olivier et al. (2002) as well as conventional shock tubes Schmidt et al. (2013). The interaction of the detonation wave with an interface is crucial but only one component of the operation; a full unsteady gas dynamic simulation of the wave propagation processes is required to predict the performance.

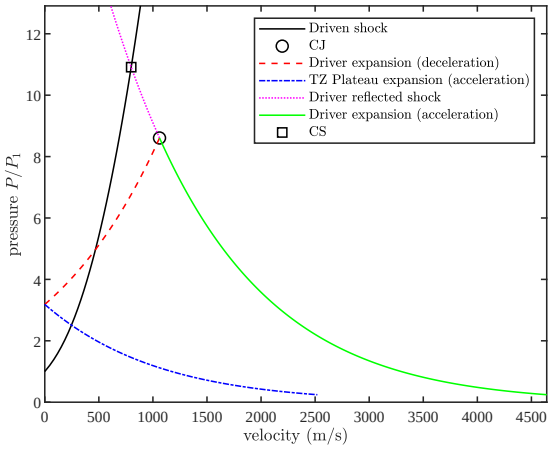

Figure 7.20: Pressure-velocity solution for forward detonation and reflected shock solutions in driver. Stoichiometric propane-oxygen driver at 0.25 atm, air at 1 atm in driven section.

Chapter 8

Numerical Methods for the Jump Equations

The most common predictive problem in shock physics is to numerically determine the post-shock state 2 given an initial state 1 and shock velocity $U_s = \mathrm{w}_1$. There are many methods to accomplish this task, two of which are given below. The first method is based on functional iteration in a single variable (density ratio). The second method is based on a two-variable (temperature and volume) implicit solution using Newton's method. The second method is more robust than the first and is used in the numerical algorithms in our software package. In order to use these methods, an equation of state in the form $e(P, \rho)$ or equivalently $h(p, \rho)$ is required. This can be either an analytic formula, a set of tabulated data, or an algorithmic procedure.

8.1 Iterative Solution with Density

One convenient way to approach this problem is to rewrite the momentum and energy jump relationships as a function of density ρ_2

$$P_2 = P_1 + \rho_1 \mathrm{w}_1^2 \left[1 - \frac{\rho_1}{\rho_2}\right] \tag{8.1}$$

$$h_2 = h_1 + \frac{1}{2}\mathrm{w}_1^2 \left[1 - \left(\frac{\rho_1}{\rho_2}\right)^2\right] \tag{8.2}$$

Using an assumed value of $\rho_2 = \rho_2^*$ and the initial state (P_1, ρ_1, h_1, w_1), Equations (8.1) and (8.2) are used to predict interim values of pressure and enthalpy, P_2^* and h_2^*. The enthalpy from (8.2) is then compared with the value obtained from the equation of state

$$h = h(P_2^*, \rho_2^*) \tag{8.3}$$

to obtain an error

$$Err = h(8.3) - h(8.2) \tag{8.4}$$

Depending on the sign of Err, a new value for $\rho_2 = \rho_2^*$ that will reduce the magnitude of Err is selected. Through repeated[1] trials (iterations), Err can be reduced to less than a desired tolerance ϵ. This formulation of the problem can be used with any equation of state that can be evaluated to yield $h(P, \rho)$; *Mollier* charts and tables (Reynolds, 1979) that are widely available for many substances are well suited for this approach. This method is the basis of the post-shock state solution in the original detonation structure program ZND developed by Shepherd (1986).

[1] This is most conveniently carried out using one of the "canned" nonlinear root solvers available in standard libraries of numerical subroutines (Press et al., 1986).

Algorithm

The details of the solution algorithm are as follows:

1. Define known quantities: Upstream state (1), e.g., specify (w_1, P_1, T_1, $\mathbf{Y}_1$), error tolerances
2. Seek unknown quantities: Downstream State (w_2, P_2, T_2, $\mathbf{Y}_2$)
3. Define the unknown specific volume ratio to be X

$$X = \frac{\rho_1}{\rho_2} \tag{8.5}$$

4. Guess a value for X within assumed upper and lower bounds $X_{min} < X < X_{max}$. As discussed below, the value of X_{min} has to be selected carefully to avoid having the solution compute nonphysical values of properties which will result in runtime errors and a failure to obtain a solution.

$$X_{min} = \frac{1}{5} \tag{8.6}$$

$$X_{max} = \frac{1}{1.005} \tag{8.7}$$

5. Compute the tentative value for pressure from momentum jump

$$P_2^* = P_1 \rho_1 \mathrm{w}_1^2 \left(1 - X\right) \tag{8.8}$$

6. Compute enthalpy from the equation of state using an assumed (frozen) or computed (equilibrium) composition $\mathbf{Y}$

$$\rho_2^* = \frac{\rho_1}{X} \tag{8.9}$$

$$h_2^* = h(P_2^*, \rho_2^*, \mathbf{Y}_2^*) \tag{8.10}$$

7. Compute the enthalpy using the energy jump equation

$$h_2 = h_1 + \frac{\mathrm{w}_1^2}{2}\left(1 - X^2\right) \tag{8.11}$$

8. Find the error as the difference between the two enthalpies

$$Err = h_2 - h_2^* \tag{8.12}$$

   In (8.10), $h(P, \rho, \mathbf{Y})$ is the thermodynamic equation of state of the products. If the products are in chemical equilibrium, in step 6, this will require determining the equilibrium composition $\mathbf{Y}_{2,eq}$ corresponding to P^* and ρ^*. This solution algorithm is valid for a general equation of state and can be simplified for an ideal gas by computing temperature as an intermediate variable in step 6.

9. Iterate until Err (8.12) is less than the specified value.
10. Return final post-shock state (2).

The program ZEROIN (Shampine and Watts, 1970) was used in Shepherd (1986) to carry out the iteration.

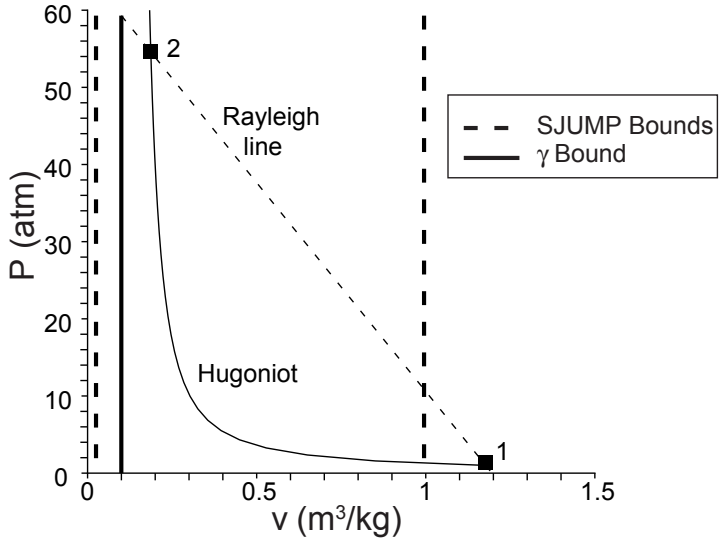

Figure 8.1: The Rayleigh line and reactant (frozen) Hugoniot with the minimum (8.6) and maximum (8.7) density ratios superimposed for stoichiometric hydrogen-air with the same initial conditions as Fig. 6.3 and a shock speed of $1.4U_{\mathrm{CJ}}$. The proposed asymptote (8.14), γ bound, is also shown. demo_RH.m

Algorithm Analysis

This algorithm has difficulty converging with strong shock waves such as the leading shock of a highly overdriven detonation, i.e., a wave speed significantly exceeding the Chapman-Jouguet value. This is due to the vertical asymptote of the Hugoniot at high pressures (Fig. 8.1). Small changes in density correspond to large changes in pressure, and if the bounds on the density are not chosen carefully, the algorithm will pick values that fall to the left of the asymptote which may cause the root-solving routine to fail. In order to use this method, we need to find a good approximation to the lower bound on the specific volume ratio X_{min}. An approximate asymptote (8.14) can be determined from the constant c_P analytic solution to the jump conditions (see Appendix A.1).

$$\frac{\rho_2}{\rho_1} = \frac{\gamma + 1}{\gamma - 1 + \dfrac{2}{M_1^2}} \tag{8.13}$$

where γ is the ratio of specific heats, c_P/c_v. As $M \to \infty$, this expression becomes

$$\frac{\rho_2}{\rho_1} = \frac{\gamma + 1}{\gamma - 1} \tag{8.14}$$

In general, particularly when considering a wide range of shock speeds, the value of $\gamma(T)$ shown (Fig. 8.2) varies with postshock temperature (and pressure for reacting cases) since $c_P(T)$. In order for this estimate to be useful, we need a value for γ. This will depend on the postshock temperature and pressure. A typical maximum leading shock velocity in unstable detonations (Eckett et al., 2000) is about $1.4U_{\mathrm{CJ}}$, where U_{CJ} is the Chapman-Jouguet value. The value of γ for a shock of this strength in air is about 1.3. Figure 8.1 shows the typical bounds on the density ratio for this case and we see that the simple estimate falls to the left[2] of the actual solution, which means that considerable trial and error is needed to get appropriate bounds on the trial value of the density. For this reason, functional iteration on density is not a very robust method for a wide range of problems, and a more reliable technique is needed.

[2]When the specific heat is a function of temperature, even if the composition is fixed, (8.14) is incorrect.

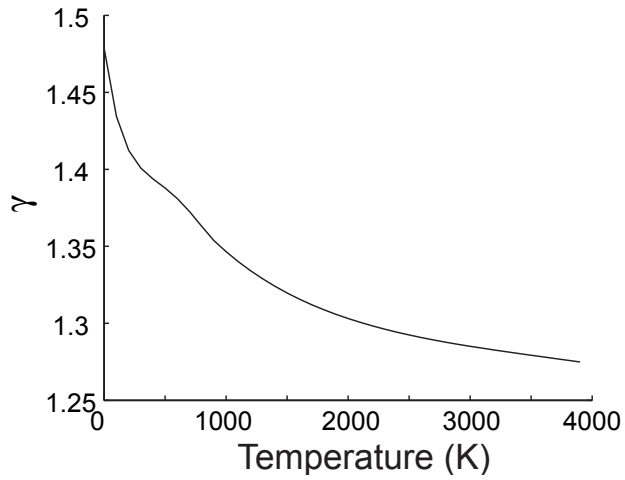

Figure 8.2: γ as a function of temperature for stoichiometric hydrogen-air at 1 atm (frozen composition).

8.2 Newton-Raphson Method in Temperature and Volume

The iterative solution with density requires a good initial guess for the density and care must be taken not to exceed the maximum density. The steep slope of the Hugoniot for strong shocks makes this method unsuitable in those cases. We have found that a more robust method is to use a two-variable Newton-Raphson scheme with the variables temperature and specific volume. The scheme presented below is an extension of the method used by Reynolds (1986) to solve the jump conditions for a Chapman-Jouguet detonation.

The momentum and energy jump conditions can be expressed as

$$\mathcal{H} = \left(h_2 + \frac{1}{2}\mathrm{w}_2^2\right) - \left(h_1 + \frac{1}{2}\mathrm{w}_1^2\right) \tag{8.15}$$

$$\mathcal{P} = \left(P_2 + \rho_2 \mathrm{w}_2^2\right) - \left(P_1 + \rho_1\ \mathrm{w}_1^2\right) \tag{8.16}$$

The exact solution to the jump conditions then occurs when both $\mathcal{H}$ and $\mathcal{P}$ are identically zero. We can construct an approximate solution by simultaneously iterating these two equations until $\mathcal{H}$ and $\mathcal{P}$ are less than a specified tolerance. An iteration algorithm can be developed by considering trial values of (T, v) for the downstream thermodynamic state 2 that are close to but not equal to the exact solution, (T_2, v_2). The expansion of (8.16) and (8.15) to first order in a Taylor series about the exact solution,

$$\mathcal{H}(T, v) = \mathcal{H}(T_2, v_2) + \frac{\partial \mathcal{H}}{\partial T}(T - T_2) + \frac{\partial \mathcal{H}}{\partial v}(v - v_2) + \ldots \tag{8.17}$$

$$\mathcal{P}(T, v) = \mathcal{P}(T_2, v_2) + \frac{\partial \mathcal{P}}{\partial T}(T - T_2) + \frac{\partial \mathcal{P}}{\partial v}(v - v_2) + \ldots \tag{8.18}$$

Recognizing that $\mathcal{H}(T_2, v_2) = \mathcal{P}(T_2, v_2) = 0$, this can be written as a matrix equation

$$\begin{bmatrix} \mathcal{H} \\ \mathcal{P} \end{bmatrix} = \begin{bmatrix} \dfrac{\partial \mathcal{H}}{\partial T} & \dfrac{\partial \mathcal{H}}{\partial v} \\ \dfrac{\partial \mathcal{P}}{\partial T} & \dfrac{\partial \mathcal{P}}{\partial v} \end{bmatrix} \begin{bmatrix} \delta T \\ \delta v \end{bmatrix} \tag{8.19}$$

where $\delta T = T - T_2$ and $\delta v = v - v_2$. This equation is used to compute corrections, δT and δv, to the current values of (T, v) and through successive applications, approach the true solution to within a specified error tolerance. At step i, we have values (T^i, v^i) which we use to evaluate (8.15) and (8.16) and obtain $\mathcal{H}^i$ and $\mathcal{P}^i$; then we solve (8.19) for δT^i and δv^i and compute the next approximation to the solution as

$$T^{i+1} = T^i - \delta T^i \tag{8.20}$$

$$v^{i+1} = v^i - \delta v^i \tag{8.21}$$

The corrections can be formally obtained by inverting the Jacobian

$$J = \begin{bmatrix} \dfrac{\partial \mathcal{H}}{\partial T} & \dfrac{\partial \mathcal{H}}{\partial v} \\ \dfrac{\partial \mathcal{P}}{\partial T} & \dfrac{\partial \mathcal{P}}{\partial v} \end{bmatrix} \tag{8.22}$$

and carrying out the matrix multiplication operation.

$$\begin{bmatrix} \delta T \\ \delta v \end{bmatrix} = J^{-1} \begin{bmatrix} \mathcal{H} \\ \mathcal{P} \end{bmatrix} \tag{8.23}$$

This is equivalent to the Newton-Raphson method (Press et al., 1986) of solving systems of nonlinear equations. The derivatives needed for the Jacobian might be computed analytically although it is often simpler to compute these numerically for complex equations of state or problems that involve chemical equilibrium. This is the approach used by Reynolds (1986) in his implementation of this method for finding CJ states for detonations and the basis for the method used in the present software. The algorithms for both the Python and MATLAB implementations are essentially identical and are described next.

Subfunctions `shk_calc` and `shk_eq_calc`

The algorithms for both frozen and equilibrium shocks are formally identically and only differ in how state 2 (postshock state) is updated. For `shk_calc` the composition is kept frozen (equal to that of state 1) and for `shk_eq_calc`, the composition is equilibrated at the given thermodynamic state in order to determine state 2 thermodynamic properties.

1. Define known quantities: Upstream state (1), e.g., specify (w_1, P_1, T_1, $\mathbf{Y}_1$), error tolerances (defaults are set in software), and initial increment values (δT, δv).

2. Establish preliminary guess ($i = 1$) for downstream state (2) based on an assumed value of $\rho_2 = \rho_2^\circ$. A standard starting value that (set in the `SDTconfig` files) is $\rho_2^\circ = 5\rho_1$. This value may not work for all cases and some experimentation may be needed to find an appropriate value.

3. Compute downstream state (2) using jump conditions and current value of ρ_2^i

$$v_2^i = \frac{1}{\rho_2^i}$$

$$P_2^i = P_1 + \rho_1 \mathrm{w}_1^2 \left(1 - \frac{\rho_1}{\rho_2^i}\right)$$

4. Compute downstream temperature from the equation of state in the form

$$T_2^i = T(P_2^i, \rho_2^i, \mathbf{Y}_2^i)$$

   For frozen shocks, the downstream composition is fixed $\mathbf{Y}_2^i = \mathbf{Y}_1$, for equilibrium postshock states, the equilibrium composition $\mathbf{Y}_{2,eq}^i$ will need to determined as a function of (P_2^i, ρ_2^i). In the case of an ideal gas, a useful shortcut is to introduce an estimated temperature because the equilibrium algorithms converge most rapidly with temperature and pressure (or density) as the state variables.

5. Call Subfunction FHFP to get $\mathcal{H}(T_2^i)$ and $\mathcal{P}(T_2^i)$
6. Perturb temperature holding volume fixed and call Subfunction FHFP to get $\mathcal{H}(T_2^i+\Delta T)$ and $\mathcal{P}(T_2^i+\Delta T)$ using a suitably small perturbation ΔT
7. Perturb specific volume holding temperature fixed and call Subfunction FHFP to get $\mathcal{H}(v_2^i+\Delta v)$ and $\mathcal{P}(v_2^i+\Delta v)$ using a suitably small perturbation Δv
8. Evaluate the elements of the Jacobian by first order differences

$$\frac{\partial \mathcal{H}}{\partial T} = \frac{\mathcal{H}(T_2^i+\Delta T)-\mathcal{H}(T_2^i)}{\Delta T}$$
$$\frac{\partial \mathcal{P}}{\partial T} = \frac{\mathcal{P}(T_2^i+\Delta T)-\mathcal{P}(T_2^i)}{\Delta T}$$
$$\frac{\partial \mathcal{H}}{\partial v} = \frac{\mathcal{H}(v_2^i+\Delta v)-\mathcal{H}(v_2^i)}{\Delta v}$$
$$\frac{\partial \mathcal{P}}{\partial v} = \frac{\mathcal{P}(v_2^i+\Delta v)-\mathcal{P}(v_2^i)}{\Delta v}$$

9. Solve the linear system given in (8.19) to find δT and δv
10. Limit the values of δT and δv to avoid runtime errors.
    - δT: IF $|\delta T| > 0.2 * T_2^i$, THEN $\delta T \leftarrow 0.2 * T_2^i * \text{sgn}(\delta T)$
    - δv:
      - IF $|\delta v| > 0.2 * v_2^i$ and $v_2^i + \delta v < v_1$, THEN $\delta v \leftarrow 0.2 * v_2^i * \text{sgn}(\delta v)$
      - IF $|\delta v| > 0.5(v_1 - v_2^i)$ and $v_2^i + \delta v > v_1$, THEN $\delta v \leftarrow 0.5(v_1 - v_2^i) * \text{sgn}(\delta v)$
11. Update post-shock state

$$T_2^{i+1} = T_2^i - \delta T$$
$$v_2^{i+1} = v_2^i - \delta v$$

12. Check convergence

$$T_2^{i+1} - T_2^i < T_{error}$$
$$v_2^{i+1} - v_2^i < v_{error}$$

13. Repeat 5-12 as needed
14. Return final values of T_2 and v_2 as the post-shock state.

Subfunction FHFP

The purpose of this routine is to compute the error in jump conditions given the current state of the iteration.

Procedure:

1. Inputs:
   Upstream State (P_1, ρ_1, h_1, w_1);
   Current Guess State (P_2^i, ρ_2^i, h_2^i)
2. Determine w_2 and compute $\mathcal{H}$ and $\mathcal{P}$

$$\text{w}_2^2 = \text{w}_1^2 \left(\frac{\rho_1}{\rho_2^i}\right)^2 \tag{8.24}$$
$$\mathcal{H} = \left(h_2^i + \frac{1}{2}\text{w}_2^2\right) - \left(h_1 + \frac{1}{2}\text{w}_1^2\right) \tag{8.25}$$
$$\mathcal{P} = \left(P_2^i + \rho_2^i \text{w}_2^2\right) - \left(P_1 + \rho_1 \text{w}_1^2\right) \tag{8.26}$$

8.3 Chapman-Jouguet Detonation Velocity

As discussed previously, the (upper) Chapman-Jouguet detonation velocity, $U_{\rm CJ}$, can be determined either by finding the minimum speed solution of the jump conditions or the downstream sonic flow solution in the wave-fixed frame. The minimum wave speed method is more robust since it does not require an additional iteration to compute the equilibrium sound speed. However, obtaining an accurate solution requires careful treatment of the iteration convergence. If a robust method of computing the equilibrium sound speed is available as a standard routine, then the sonic flow method is easier to implement and test convergence. We describe both methods but in the current version of the toolbox, only the minimum wave speed method is implemented in the toolbox.

Sonic Flow Algorithm

This algorithm finds the solution of the shock jump conditions (8.15) and (8.16) where w_1 is unknown and w_2 is the equilibrium sound speed. The equilibrium sound speed is calculated by numerical evaluation of the derivative

$$a_{eq}^2 = \left(\frac{\partial P}{\partial \rho}\right)_{s\mathbf{Y}^{eq}}$$

using the methods described in Chapter 7.10.

The algorithm for computing the CJ solution is:

1. Define known quantities: Upstream state, e.g., specify $(P_1,\, T_1,\, \mathbf{Y}_1)$. Guess the downstream state, e.g., specify $(P_2^i,\, T_2^i,\, \mathbf{Y}_2^i)$ - a constant volume explosion state is a useful starting point.

2. Estimate w_1 using the guessed state 2 and equilibrium sound speed.

$$\mathrm{w}_2^i = a_{2,eq}(P_2^i, T_2^i,\ \mathbf{Y}_2^i) \tag{8.27}$$

   Evaluate the densities in state 1 and 2 and compute the associated trial value of w_1

$$\mathrm{w}_1^i = \mathrm{w}_2^i \frac{\rho_2^i}{\rho_1} \tag{8.28}$$

3. Evaluate the enthalpy in states 1 and 2 and compute jump errors $\mathcal{H}$ and $\mathcal{P}$

$$\mathcal{H} = \left(h_2^i + \frac{1}{2}a_{2,eq}^{i,2}\right) - \left(h_1 + \frac{1}{2}\mathrm{w}_1^{i,2}\right) \tag{8.29}$$

$$\mathcal{P} = \left(P_2^i + \rho_2^i a_{2,eq}^{i,2}\right) - \left(P_1 + \rho_1 \mathrm{w}_1^{i,2}\right) \tag{8.30}$$

4. Use a root-finding method to iterate on temperature and pressure of CJ state to reduce the residuals $\mathcal{H}$ and $\mathcal{P}$ below the desired error tolerances.

This method was explored in the orginal toolbox and worked well for simple mixtures, however, there were difficulties with mixtures that have a large number of product species in converging to an equilibrium sound speed. The method has been revised[3] and an improved version has been implemented as an option in the latest toolbox.

Minimum Wave Speed Algorithm

As discussed previously, the minimum wave speed solution uniquely determines the (upper) Chapman-Jouguet point. We implement this by determining w_1 as a function of the density ratio ρ_2/ρ_1 at discrete points and then using a combination of analysis near the CJ point and statistical methods, find an approximation

[3]The new algorithm was developed by Zifeng Wang of Tsinghua University in 2021.

to the minimum value of w_1. The solution of the jump conditions for a given density uses the same Newton-Raphson method previously discussed but with a key difference that instead of solving a system of equations in volume and temperature (8.19), we used initial velocity and temperature as variables.

$$\begin{bmatrix} \mathcal{H} \\ \\ \mathcal{P} \end{bmatrix} = \begin{bmatrix} \dfrac{\partial \mathcal{H}}{\partial T} & \dfrac{\partial \mathcal{H}}{\partial \mathrm{w}_1} \\ \\ \dfrac{\partial \mathcal{P}}{\partial T} & \dfrac{\partial \mathcal{P}}{\partial \mathrm{w}_1} \end{bmatrix} \begin{bmatrix} \delta T \\ \\ \delta \mathrm{w}_1 \end{bmatrix} \tag{8.31}$$

The minimum wave speed solution is carried out with two routines. The routine `CJ_calc` computes the wave speed or shock velocity consistent with the jump conditions and corresponding to a trial value of downstream density. The routine `CJspeed` iterates on the trial density, calling `CJ_calc` repeatedly and determining the CJ velocity as the minimum value of the wave speed.

Subfunction `CJ_calc`

The purpose of this routine is to compute a shock velocity that is consistent with a given upstream state and a specified downstream density. The solution w_1 will be greater than or equal to the CJ speed.

1. Define known quantities: Upstream State, e.g., (P_1, ρ_1, $\mathbf{Y}_1$) and downstream density ratio ρ_2, error tolerances, increment values (δT, $\delta \mathrm{w}_1$)
2. Seek unknown quantities: Downstream State (P_2, T_2, $\mathbf{Y}_2$) and value of shock speed w_1.
3. Establish preliminary guess: ($i = 1$)
$$\mathrm{w}_1^i = 2000$$
$$T_2^i = 2000$$
4. Equilibrate the system with constant temperature and specific volume to find P_2^i and h_2^i
5. Call Subfunction `FHFP` to get $\mathcal{H}(T_2^i)$ and $\mathcal{P}(T_2^i)$
6. Perturb temperature holding initial velocity constant and call Subfunction `FHFP` to get $\mathcal{H}(T_2^i + \Delta T)$ and $\mathcal{P}(T_2^i + \Delta T)$ with a suitably small value of ΔT
7. Perturb initial velocity holding temperature constant and call Subfunction `FHFP` to get $\mathcal{H}(\mathrm{w}_1^i + \Delta \mathrm{w}_1)$ and $\mathcal{P}(\mathrm{w}_1^i + \Delta \mathrm{w}_1)$ with a suitably small value of $\Delta \mathrm{w}_1$
8. Evaluate the elements of the Jacobian by first order differences a
$$\frac{\partial \mathcal{H}}{\partial T} \approx \frac{\mathcal{H}(T_2^i + \Delta T) - \mathcal{H}(T_2^i)}{\Delta T}$$
$$\frac{\partial \mathcal{P}}{\partial T} \approx \frac{\mathcal{P}(T_2^i + \Delta T) - \mathcal{P}(T_2^i)}{\Delta T}$$
$$\frac{\partial \mathcal{H}}{\partial \mathrm{w}_1} \approx \frac{\mathcal{H}(\mathrm{w}_1^i + \Delta \mathrm{w}_1) - \mathcal{H}(\mathrm{w}_1^i)}{\Delta \mathrm{w}_1}$$
$$\frac{\partial \mathcal{P}}{\partial \mathrm{w}_1} \approx \frac{\mathcal{P}(\mathrm{w}_1^i + \Delta \mathrm{w}_1) - \mathcal{P}(\mathrm{w}_1^i)}{\Delta \mathrm{w}_1}$$
9. Solve the linear system given in (8.31) to find δT and $\delta \mathrm{w}_1$
10. Limit the value of δT
IF $|\delta T| > 0.2 * T_2^i$, THEN $\delta T = 0.2 * T_2^i * \mathrm{sgn}(\delta T)$
11. Update values
$$T_2^{i+1} = T_2^i - \delta T$$
$$\mathrm{w}_1^{i+1} = \mathrm{w}_1^i - \delta \mathrm{w}_1$$

12. Equilibrate the system with constant temperature and specific volume to find P_2^{i+1} and h_2^{i+1}
13. Check convergence

$$T_2^{i+1} - T_2^i < T_{error}$$
$$\mathrm{w}_1^{i+1} - \mathrm{w}_1^i < \mathrm{w}_{1error}$$

The values of the error bounds are determined by using the error tolerances (`ERRFT,ERRFV`) multiplied by the current values of temperature and velocity so the convergence is obtained by reducing the relative error to less than the values of `ERRFT,ERRFV`.

14. Repeat 4-13 as needed
15. Return final values of T_2 and w_1.

Minimizing Initial Velocity

Following the algorithm outlined above, we are able to find how the initial velocity varies with the final density. Analytically, we have found that the initial velocity varies quadratically with density close to the CJ point (see Appendix B). In order to find the minimum w_1, the CJ speed, in MATLAB we use `cfit` toolbox and in Python we have implemented the analytical solution for a quadratic least squares fit to the data points that we gathered from the above algorithm. We use the R-squared value to quantify the precision of our fit and simultaneously obtain observation prediction bounds to quantify the uncertainty in our minimum wave speed.

Subfunction `CJspeed`

The purpose of this routine is to compute the CJ speed by minimizing the wave speed as a function of downstream density.

1. Define known quantities: Upstream State, e.g., (P_1, T_1, $\mathbf{Y}_1$), initial ($i = 1$) guess for density ratio $X = \rho_2/\rho_1$ and range ($X_{min}^i = 1.5$, $X_{max}^i = 2.0$) of interest for the solution. The default values of the range limits and number of values ((`numsteps`=20) of X are hardcoded but usually adequate for most gas detonations.
2. Seek unknown quantities: CJ speed
3. Call `CJ_calc` for each density ratio, X_i for $i \in (0, \text{numsteps})$)
4. Fit data to a quadratic equation ($aX^2 + bX + c$) using the method of least squares (regression)
5. Find minimum of fit $\left(X_{min} = -\dfrac{b}{2a}\right)$
6. Narrow density ratio range

$$X_{min}^{i+1} = X_{min} - 0.001X_{min} \tag{8.32}$$
$$X_{max}^{i+1} = X_{min} + 0.001X_{min} \tag{8.33}$$

7. Check convergence using the regression coefficient of determination "R-squared" (R^2). For convergence require that:

$$R^2 > 0.99999\ . \tag{8.34}$$

8. Repeat 3-7 as needed
9. Return the final result when convergence is obtained. The predicted CJ speed is computed from the coefficients

$$\mathrm{w}_{1min} = \frac{b^2}{4a} - \frac{b^2}{2a} + c \tag{8.35}$$

of the fitted curve and the prediction bounds on this minimum are given by the descriptive statistics for the curve fit.

Figures 8.3 and 8.4 depict the results that we obtain from the method described in this section.

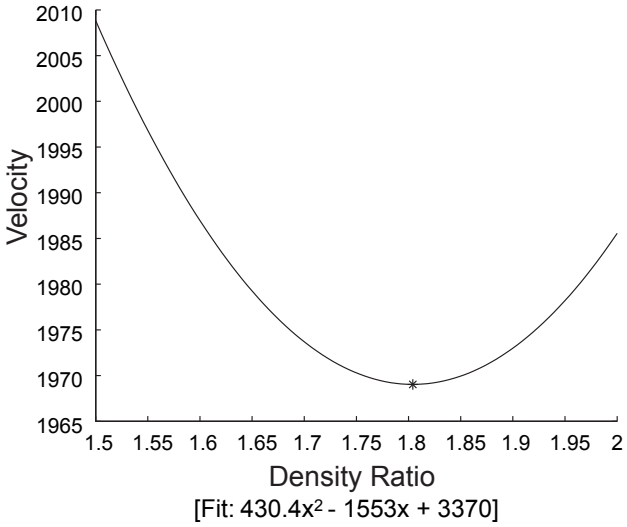

Figure 8.3: Initial velocity as a function of density ratio for stoichiometric hydrogen-air with intial temperature 300 K and initial pressure 1 atm. Chapman-Jouguet velocity is 1969.03 m/s corresponding to a density ratio of 1.80. demo_CJ.m

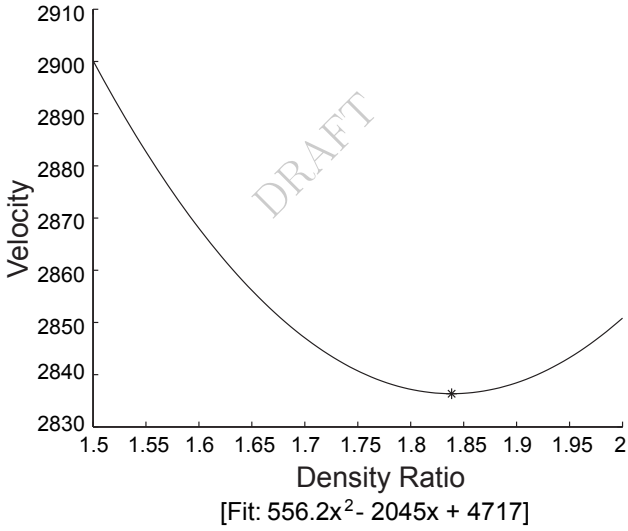

Figure 8.4: Initial velocity as a function of density ratio for stoichiometric hydrogen-oxygen with intial temperature 300 K and initial pressure 1 atm. Chapman-Jouguet velocity is 2836.36 m/s corresponding to a density ratio of 1.84. demo_CJ.m

Statistical Analysis of CJ Speed Solution

As discussed above, we have used the R-squared value to quantify the precision of the fit and quantify the uncertainty in the computed value of the CJ speed. In this section these aspects will be discussed more completely.

If $y(x)$, the R-squared value is defined by the following equation

$$R^2 = \frac{\sum_{i=1}^{n} (\hat{y}_i - \overline{y})^2}{\sum_{i=1}^{n} (y_i - \overline{y})^2} \tag{8.36}$$

If this value is very close to unity then the curve is a good fit.

Simultaneous prediction bounds measure the confidence that a new observation lies within the interval regardless of the predictor value. There are two main measures of confidence: confidence bounds and prediction bounds. The confidence bounds give the uncertainty in the least square coefficients. These uncertainties are correlated, and the prediction bounds account for this correlation. In our particular problem we have uncertainty in both the x value of the minimum as well as the y value of the minimum. This is because we choose

$$x_{min} = -\frac{b}{2a} \tag{8.37}$$

$$y_{min} = ax_{min}^2 + bx_{min} + c \tag{8.38}$$

and there is uncertainty in a, b, and c. We choose simultaneous prediction bounds because that will account for the uncertainty in x. Non-simultaneous prediction bounds assume that there is no uncertainty in x. MATLAB defines simultaneous new observation prediction bounds with the following expression.

$$P_{s,o} = \hat{y} \pm f\sqrt{\sigma_{sample}^2 + xSx'} \tag{8.39}$$

In this expression f is the inverse of the cumulative distribution function F (Fig. 8.5), σ_{sample}^2 is the mean squared error (8.40), x is the predictor value for the new observation, and S is the covariance matrix of the coefficient estimates (8.41).

$$\sigma_{sample}^2 = \frac{1}{\nu}\sum_{i=0}^{n}(y_i - \hat{y}_i)^2 \tag{8.40}$$

$$S = (X^T X)^{-1}\sigma_{sample}^2 \tag{8.41}$$

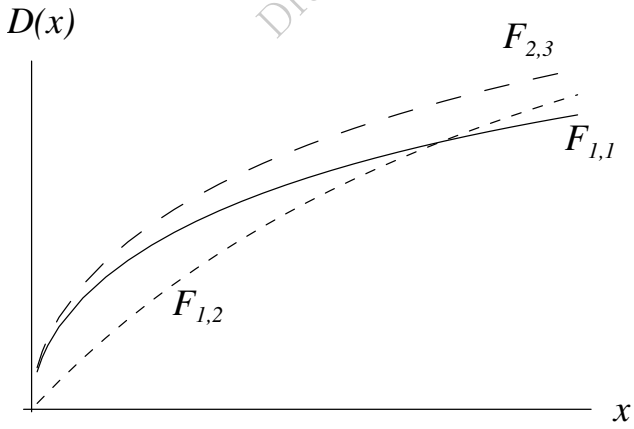

Figure 8.5: Cumulative distribution function F for error in fitted parameters.

8.4 Verification and Convergence

As depicted in Fig. 6.3, for a Chapman-Jouguet detonation in stoichiometric hydrogen-air with standard intial conditions, there is a unique post-shock state. Our experience is that unique results are obtained for all cases of equilibrium reacting gas mixtures described by ideal gas thermodynamics.[4] Theoretical support

[4]This does not mean that the ideal post-shock state or CJ condition always correctly describes the physical situation. We are only referring to the mathematical uniqueness of our solution methods.

for the uniqueness of the post-shock state is given by Menikoff and Plohr (1989). They have determined that the Bethe-Weyl theorem assures that the Hugoniot is well-behaved when Γ, the fundamental derivative of gas dynamics, is positive. We note that our algorithms may not be appropriate for cases when $\Gamma < 0$.

We can verify the correctness of the software by comparing with perfect gas analytic solutions and validating it against results from legacy software. First, we can compare `PostShock_fr` results with the exact solution to the jump conditions for a perfect gas (see Thompson (1972) or Appendix A.1).

$$P_2 = P_1 \left[1 + \frac{2\gamma}{\gamma + 1} \left(M_1^2 - 1 \right) \right] \tag{8.42}$$

$$v_2 = v_1 \left[1 - \frac{2}{\gamma + 1} \left(1 - \frac{1}{M_1^2} \right) \right] \tag{8.43}$$

In the case of a perfect gas, the specific heat is constant and the enthalpy can be expressed as $h = c_P T$. Figure 8.6 shows the error in pressure, density, temperature, and enthalpy between the exact solution and `PostShock_fr`'s results for shock speeds ranging from 500 to 5000 m/s. The system for these simulations was one mole of Argon at 1 atmosphere and 300 Kelvin.

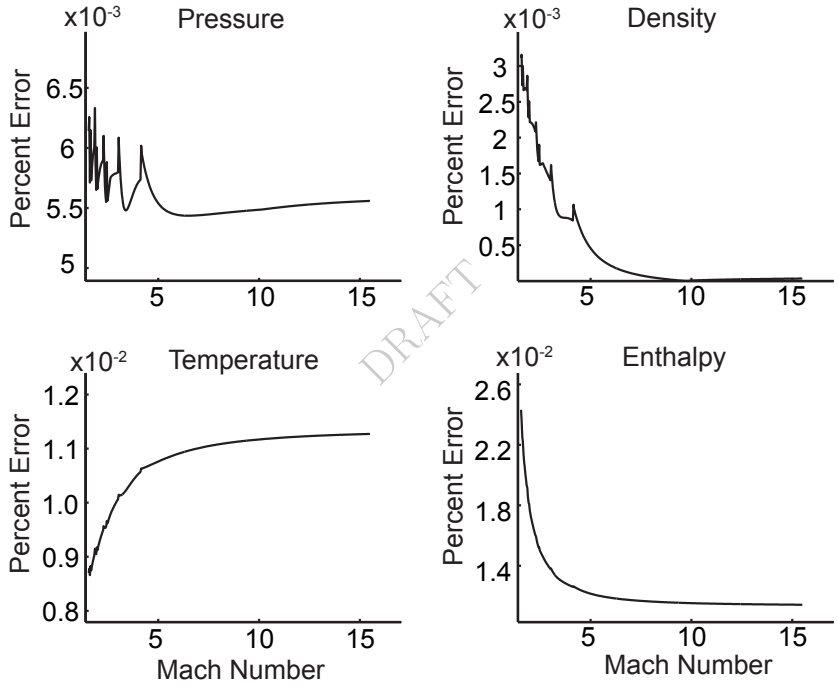

Figure 8.6: The percent error in the exact solution and the results of `PostShock_fr` for one mole of Argon with initial temperature 300 K and initial pressure 1 atm.

For mixtures with non-constant specific heat, we can compare the results of `PostShock_fr` with STANJAN (Reynolds, 1986) results. Figure 8.7 shows the percent difference in post-shock pressure and temperature for stoichiometric hydrogen air with varying shock speed.

We have also investigated the shape of the $\mathcal{H}$ and $\mathcal{P}$ surfaces resulting from `PostShock_fr`. Figure 8.8 shows that the surface generated by calculating the RMS of $\mathcal{H}$ and $\mathcal{P}$ according to (8.44) has a distinct minimum, and that the minimum corresponds to the valid solution.

$$RMSCJ = \sqrt{\left(\frac{\mathcal{H}}{h_{\mathrm{CJ}}} \right)^2 + \left(\frac{\mathcal{P}}{P_{\mathrm{CJ}}} \right)^2} \tag{8.44}$$

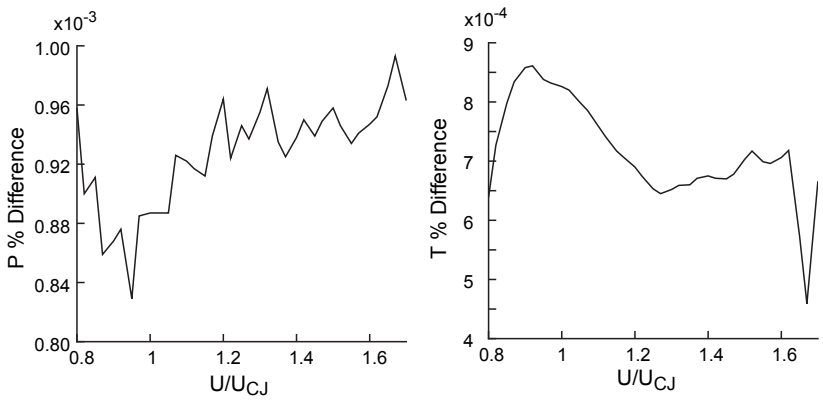

Figure 8.7: The percent difference in the solutions of STANJAN and `PostShock_fr` for hydrogen-air at an equivalence ratio of 0.5 for varying shock speed with initial temperature 300 K and initial pressure 1 atm.

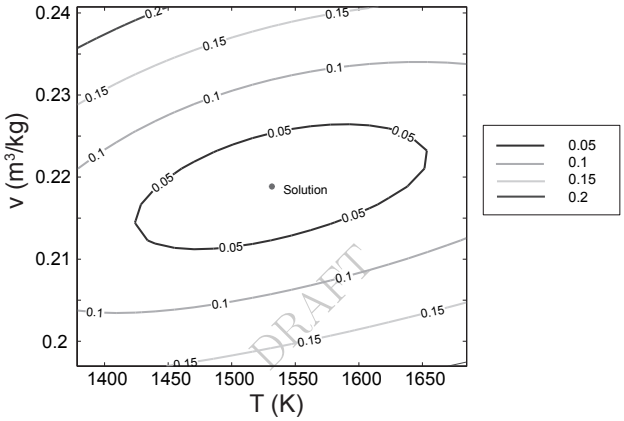

Figure 8.8: A contour plot of the RMS surface with the solution indicated at the minimum.

The concave shape of the RMS surface implies that the solution should converge to the minimum. Figure 8.9 shows the absolute value of the differential values at each step and demonstrates this convergence.

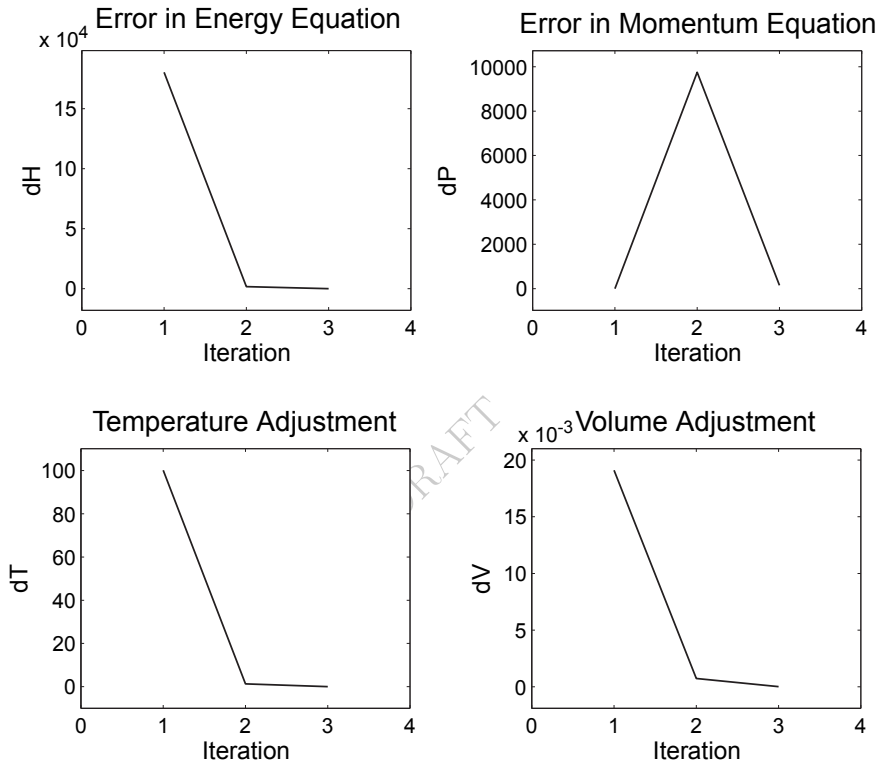

Figure 8.9: Convergence study for stoichiometric hydrogen-air with initial temperature 300 K and initial pressure 1 atm using `PostShock_fr`.

Part III

Reacting Flows

This part of these notes treats steady flows and some simple unsteady flows which are not in equilibrium or frozen and chemical reactions must be considered. The steady flows treated are the reaction zones behind shock and detonation waves moving at constant speed, the reaction zone along the stagnation streamline in supersonic blunt body flows, flow through a converging-diverging nozzle and quasi-one dimensional flows with friction and heat transfer modeled as wall functions. The unsteady flows modeled include reactions occurring under constant temperature, pressure and volume conditions or with prescribed volume or pressure time dependence.